2013 European Control Conference (ECC)
July 17-19, 2013, Zürich, Switzerland.

Pedaling Torque Reconstruction for Half Pedaling Sensor

P. Spagnol, M. Corno, S. M. Savaresi

Abstract— **Electrically Power Assisted Cycles (EPACs) have been gaining increasing attention worldwide during the past few years. Market analysis show that cyclists prefer torque assisted EPACs over velocity-based ones. A torque assisted cycle requires an estimate or measurement of the cyclist torque, which increases the cost and complexity of the set-up. Among the viable solutions, sensors mounted on the pedal axis have several advantages in terms of packaging and cost; unfortunately, they are capable of measuring the torque exerted only on one pedal. This paper deals with the development, implementation and validation of two algorithms to estimate the entire revolution torque using a half pedaling sensor. The algorithms are based on the iso-power or iso-torque assumptions (checked on a high-end training bicycle). The algorithms are validated using road measurements, showing that a sufficient level of accuracy for EPAC is reached.**

I. Introduction

Energy prices and environmental considerations have increased the interest on Light Electric Vehicles (LEVs). Strict regulations and new paradigms for urban mobility (e.g. bike and car sharing) have been introduced in urban areas in order to tackle traffic issues and pollution. In this urban context, Electrically Power Assisted Cycles (EPACs) are receiving a great deal of attention for their ease of use and cost effectiveness.

Several studies analyze the state of the art of EPACs [1] and try to predict their technical evolution based on users evaluations [2]. The consensus [2] indicates that EPACs basing the electrical assistance level on pedaling torque measurement are more appreciated in terms of cycling feeling than velocity-based EPACs.

In previous works [3], [4], a full hybrid electric bike (HEB) has been presented. Based on a State-of-Charge sustaining strategy, Bike+ increases the overall pedaling efficiency. The strategy developed in previous work is based on bicycle speed; however in some instances (initial boost and uphill pedaling), a torque-based strategy can further improve efficiency. The problem of torque measurement/estimation thus arises [5].

Bike+ (as other EPACs) is equipped with a torque sensor mounted on the bottom bracket and directly connected to the pedals. The configuration of the sensing architecture makes it so that it measures only the torque applied on the left pedal. Thus, an algorithm to estimate right torque and therefore the global torque is needed. In this paper, two such algorithms are presented. They are based on two different approximations: equal torque and equal power between the right and left pedals over one cycle. The proposed algorithms, although being based on two approximations, represent a improvement over currently employed techniques. Most of the times, in current EPACs equipped with half-pedaling sensor a low pass filter is employed to "smooth out" the blind half. This technique inevitable causes lags in the response to torque variations.

The paper is structured as follows. In Section II, a description of the sensor is presented. The architecture is presented and a simplified model employed to explain its main features is proposed. Section III details the torque reconstruction algorithms starting from some observation on a laboratory ergometer. The proposed algorithms need to be compared to a reliable measurement or estimation of the torque acting on the bike. Section IV details the methodology followed to estimate the torque starting from a longitudinal model. Results of the comparison between the reference torque and the estimate are shown in Section V.

II. Experimental Set-up

The bike used for the experimental setup is the hybrid-electric bike (HEB) described in [3]. In this work, we used the hybrid bike as a traditional bike (so without the electric aid), focusing the attention on the torque data acquired by the pedaling sensor integrated into the bottom bracket (THUN X-CELL RT).

Fig. 1 - THUN X-CELL RT sensor

This sensor is able to measure

- pedaling cadence and direction (using two digital Hall Sensors with 32 pulses per revolution);
- torque.

This sensor is widely used in commercial e-bikes thanks to its compactness and robustness. The transducer returns a voltage proportional to the measured torque (10mV/Nm). Torque is proportional to the twist of a torsional element

All the authors work at Dipartimento di Elettronica e Informazione, Politecnico di Milano, Milano, Italy spagnol@elet.polimi.it, corno@elet.polimi.it, savaresi@elet.polimi.it

placed in the middle of the torque sensor and is measured as a magnetic displacement by a Hall sensor. Considering the presence of the chain, a static model of the sensor is depicted in Fig. 2.

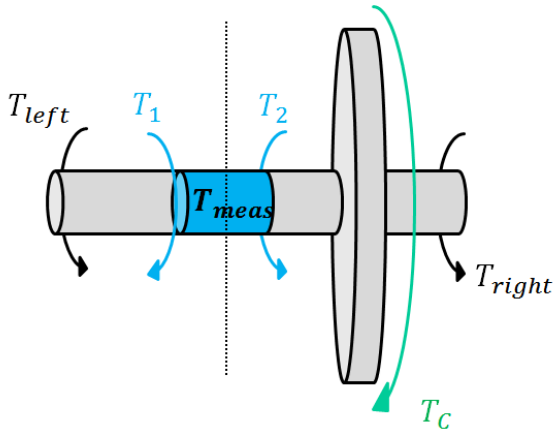

Fig. 2 - Sensor model scheme

T_{left} and T_{right} are respectively the torque applied to the left and the right pedal; T_C is the bike chain reaction; T_1 and T_2 are the torque applied to the torsional element of the sensor. T_{meas} represents the torque measured by the sensor. Static tests without the chain show that

$$T_{meas}(t) = \frac{(T_1(t) + T_2(t))}{2}. \quad (1)$$

As normally cyclists push alternatively with one or the other leg, there are two possible configurations. When torque is applied on the left pedal, the torque balance is:

$$T_{left}(t) = T_1(t); \quad (2)$$

the measuring element is fully elastic, all the torque applied on one side is transmitted to the other, so that:

$$T_1(t) = T_2(t). \quad (3)$$

Finally, the torque is transmitted to the chainwheel generating the chain reaction:

$$T_C(t) = T_2(t). \quad (4)$$

Substituting Equations (2) and (4) in (1) one can obtain:

$$T_{left}(t) = T_C(t). \quad (5)$$

Moreover, considering Equation (1) it is possible to assess that:

$$T_{meas}(t) = T_{left}(t). \quad (6)$$

On the other hand, during the right pedaling half-revolution, the torque balance is the following:

$$T_{right}(t) = T_C(t). \quad (7)$$

Thus, all the torque generated by the right leg on the pedaling shaft is applied to the chainwheel. As a consequence:

$$T_{meas}(t) = 0. \quad (8)$$

The sensor is able to catch the torque generated on the left pedal only. The right half-revolution torque is not measured due to the presence of the chainwheel, on the right part of the pedaling shaft. In Fig. 3 an example of the measured torque is shown. Some remarks can be made inspecting the torque signal:

- As expected, only the effect of one leg is measured by the sensor; as for the other leg nothing is observable;
- The measured torque dips into the negative half-plane, when the right leg is pushing. This negative torque is produced because non professional cyclists do not lift the left leg while pushing the pedal with the other [6]. Thus, the weight of the passive left leg and pedal generates a negative torque that is measured by the sensor.

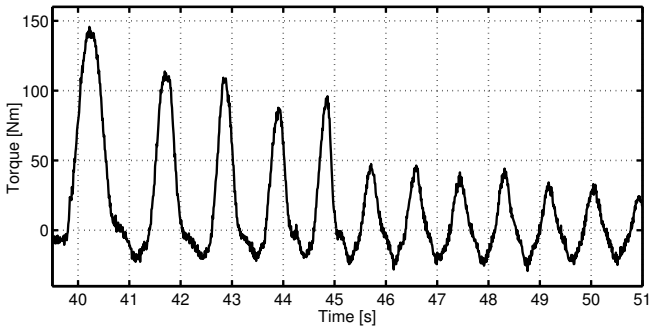

Fig. 3 - Example of measured torque during pedaling

In this work, a method for estimating the whole cyclist torque is proposed.

III. Torque Estimation Algorithms

As shown in Section II, the torque sensor is able to measure only the torque introduced by the left leg. The main focus of this work is to evaluate $T_{cyclist}$ starting from measurement similar to the one shown in Fig. 3.

In order to study the forces applied on a bike during cycling [7] and understand the behavior of the torque applied by the left and right legs, an experiment on a sport laboratory ergometer has been carried out in collaboration with Sport Service Mapei[1]. The ergometer is a fully instrumented exercise bicycle used to assess performance of professional cyclists in terms of maximal deliverable power, resistance, oxygen consumption and other important parameters. Particularly, the ergometer used for the tests is equipped with a dual torque sensor for measuring both left and right pedaling torque. Data has been analyzed in order to compare left pedaling torque with right pedaling torque. As one can see in Fig. 4 the pushes on pedals are quite symmetric.

In this work we tried to exploit this symmetry normally present during pedaling to reconstruct the unknown T_{right} measurement. There are two main symmetries to be considered:

[1] http://www.mapeisport.it/default.asp?LNG=EN

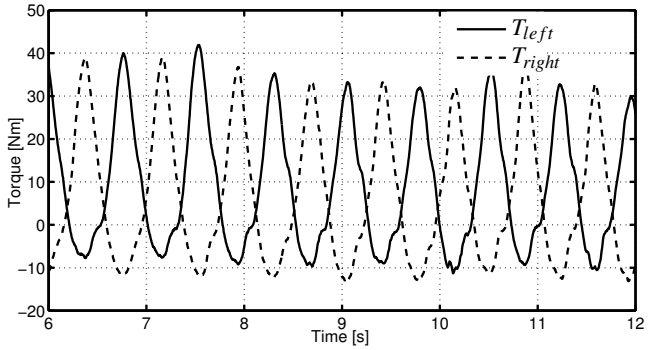

Fig. 4 - Example of measured left and right torque during ergometer test

- power symmetry;
- torque symmetry;

The analysis of the full length of the ergometer test in terms of symmetries shows that there is a strong correlation between power or torque of left and right pedaling revolution as depicted in Fig. 5.

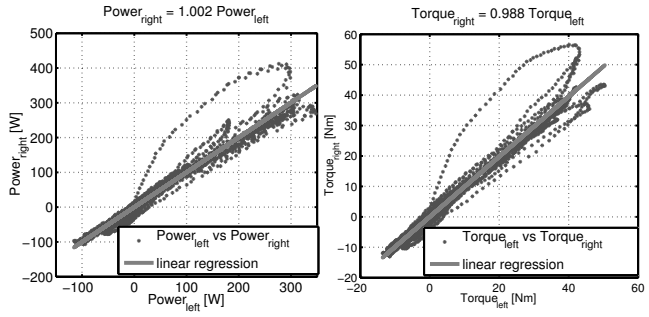

Fig. 5 - Analysis of power/torque pedaling symmetries

Two algorithms are proposed based on the above consideration. The idea is to compute the right leg torque so that either the torque profile or the power profile applied in the previous half revolution are maintained, adjusted for possible variation in speed. Two LIFO buffers are employed and a new piece of data in pushed at every sampling time. In the first buffer the pedal position $\theta \in [0, 2\pi)$ is stored, in the second either the measured torque $T_{meas}(t)$ or the computed power $P_{meas}(t) = T_{left}(t)\omega_{pedal}(t)$. Thanks to these buffers the migration from the time domain to the angular domain it is possible, so to map the applied torque (or power) onto the pedal angle.

Then, if the iso-torque hypotheses is employed, the torque is estimated by:

$$\hat{T}_{right}(t) = T_{meas}(t^\star) \text{ where } t^\star : \theta(t^\star) = \theta(t) - \pi \qquad (9)$$

Basically, the estimated right torque is equal to the torque applied by the left leg half period before.

In case of symmetric power hypothesis, a similar strategy is employed:

$$\tilde{T}_{right}(t) = \frac{P_{meas}(t^\star)}{\omega_{ped}(t)} \text{ where } t^\star : \theta(t^\star) = \theta(t) - \pi \qquad (10)$$

In this case a power balance between two time instants distant half period has been exploited in order to calculate the value of the torque developed by the right leg.

Finally,

$$\hat{T}_{pedaling}(t) = \hat{T}_{right}(t) + T_{left}(t) \qquad (11)$$

$$\tilde{T}_{pedaling}(t) = \tilde{T}_{right}(t) + T_{left}(t) \qquad (12)$$

where $\hat{T}_{pedaling}(t)$ is the total pedaling torque in case of symmetric torque hypothesis, and $\tilde{T}_{pedaling}(t)$ is the total pedaling torque in case of symmetric power hypothesis. An example of estimated pedaling torque starting from the same dataset in Fig. 3 is proposed in Fig. 6. As one can see, there are no significant differences between the two algorithms. Both strategies correctly capture the fact that there are two configurations in which no torque is delivered by the cyclist (when the pedal crank is vertical, so that the direction of the force given by the leg and the pedal "arm" are parallel).

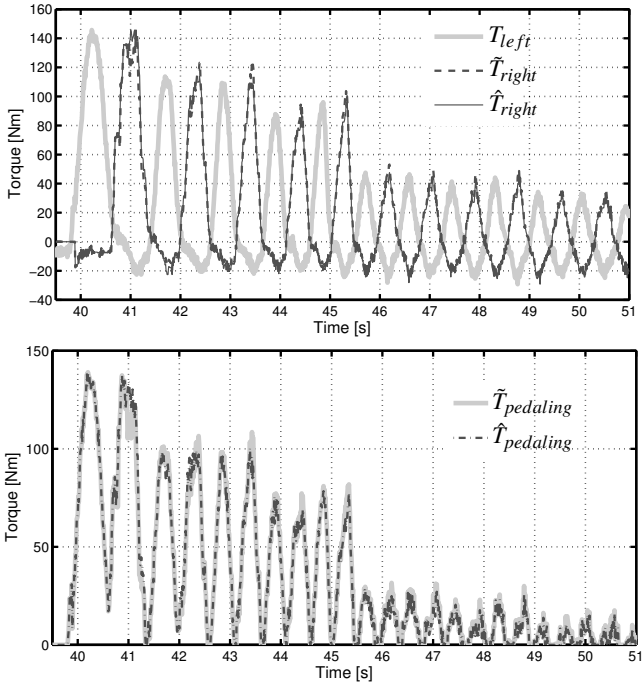

Fig. 6 - Comparison between $\hat{T}_{right}(t)$ and $\tilde{T}_{left}(t)$ and between $\hat{T}_{pedaling}(t)$ and $\tilde{T}_{pedaling}(t)$

In order to validate these two algorithms, a way to measure or calculate the real torque is needed. In the next section, a methodology to generate the reference signal is proposed.

IV. Reference Generation and Transmission Model

In order to evaluate the proposed algorithms, a measurement or reliable estimation of the real torque is needed. As a dynamometer or an alternative accurate torque sensor device - such as the one presented in [8] - are not available, a model based estimation is developed. In this work we exploit a continuously calibrated longitudinal model of the bike. The model is derived assuming a high grip surface, and

consequently neglecting slip. It is governed by the following equations:

$$\begin{cases} F_{cyclist} - F_{braking} = F_{inertia} + F_{fric} + F_{slope} \\ F_{cyclist} \geq 0 \\ F_{braking} \geq 0 \\ F_{fric} \geq 0 \end{cases} \tag{13}$$

where $F_{cyclist}$ is the force transmitted to the rear wheel by the cyclist, which is always positive. $F_{braking}$ is the force generated while using the mechanical brakes (always positive); $F_{inertia}$ is the inertial force and F_{fric} corresponds to the force needed to overcome frictions (positive). Finally F_{slope} is the force due to the presence of a slope. It can be positive going uphill or negative going downhill. In this work the tests are carried out on a flat surface without wind and with no braking, thus F_{slope} and $F_{braking}$ are neglected. Detailing the remaining terms, it is obtained

$$\begin{cases} F_{inertia} = Ma \\ F_{fric} = \alpha v^2 + \beta v + \gamma \end{cases} \tag{14}$$

where M is the (in this case known) mass of the cyclist and the bike, a is the acceleration of the bike, α, β, γ are coefficients identified during a coasting down test as shown in [9]. Finally, v is the bike speed. Substituting (14) in (13) one obtains:

$$\begin{cases} if \ F_{inertia} + F_{friction} \geq 0 \\ \quad F_{cyclist} = Ma + \alpha v^2 + \beta v + \gamma \\ \quad F_{braking} = 0 \\ else \\ \quad F_{cyclist} = 0 \\ \quad F_{braking} \geq 0 \end{cases} \tag{15}$$

The parameters have been identified with a series of coasting down tests and mass measurement, resulting in the validation shown in Fig. 7.

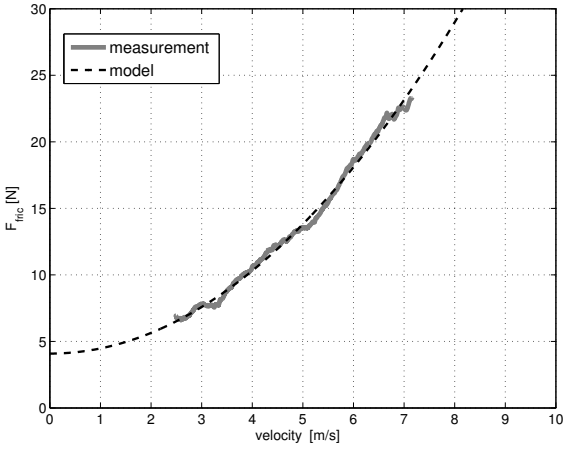

Fig. 7 - Comparison between modeled and measured F_{fric}

In order to verify the possibility to compare $F_{cyclist}$ calculated using the longitudinal model with the torque developed by pedaling an experiment pedaling only on the left pedal has been performed. According to the model the pedaling force results in:

$$F_{left} = T_{left} \frac{r}{R_w} \tag{16}$$

where F_{left} is the force developed considering r (*i.e.* the gear ratio) and R_w (*i.e.* the wheel radius). Fig. 8 shows a comparison between $F_{cyclist}$ and F_{left}. From figure it is immediately apparent that the measured force 'anticipates' the modeled force. As the model force is derived directly from acceleration, the cause is to be searched in the transmission and frame dynamics (elasticity of the sensor and pedaling shaft, chain, rear gear, wheel shaft and tire). This means that the modeled force cannot be directly employed for validation purposes; the above described dynamics has to be accounted for. A *black-box* [10] model describing the dynamics from

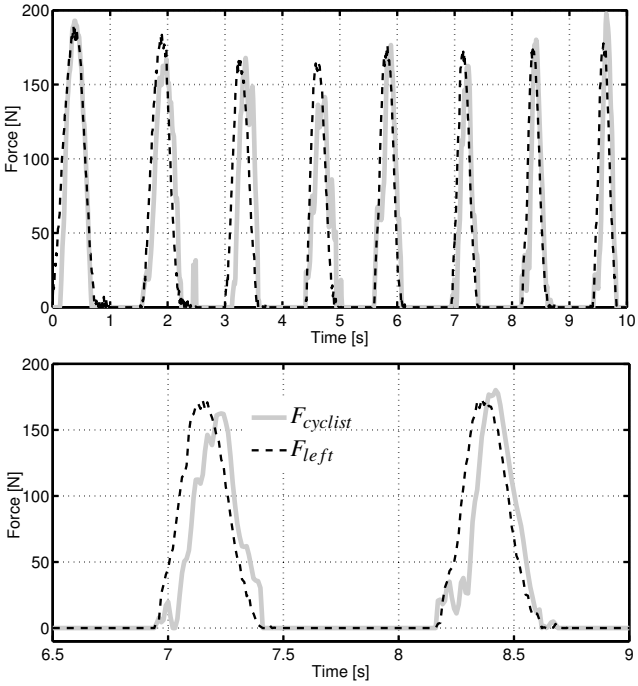

Fig. 8 - Comparison between $F_{cyclist}$ and F_{left}

pedal force, F_{left}, to cyclist force, $F_{cyclist}$, is thus identified starting from the same experiment. Three different model families are compared:

- Continuous-time linear process models (with n poles and one zero, $n \in [1..2]$).
- Discrete-time linear ARX models (with m auto-regressive coefficients and m exogenous coefficients, $m \in [1..10]$).
- Discrete-time Neural Network (NN) based models (with two auto-regressive coefficients and k layers, $k \in [1..8]$), referred to as NARX.

The models have been compared using the following

performance indexes:

$$J_{L_2^2} = \frac{\sum_{t=1}^{T}\left(F_{cyclist}(t) - \hat{F}_{cyclist}(t)\right)^2}{\sum_{t=1}^{T}\left(F_{cyclist}(t) - \left(\frac{1}{T}\sum_{i=1}^{T}F_{cyclist}(i)\right)\right)^2} \geq 0 \quad (17)$$

$$J_{RMSE} = \sqrt{\frac{1}{T}\sum_{t=1}^{T}\left(F_{cyclist}(t) - \hat{F}_{cyclist}(t)\right)^2} \quad (18)$$

Performance index (17) is a normalized squared-L_2 norm of the error: the squared distance of the model output $\hat{F}_{cyclist}(t)$ from $F_{cyclist}(t)$, normalized by the squared distance of $F_{cyclist}(t)$ from its average value. The smaller $J_{L_2^2}$, the better the model. In (18) the root mean squared error (J_{RMSE}) is considered. Table I shows the performance indexes - in validation - calculated considering the best coefficients set of each model family: the best result is given by the NN with 2 auto-regressive coefficients and 4 hidden layers.

Fig. 9 show the comparison between $\hat{F}_{cyclist}(t)$ and $F_{cyclist}(t)$ for the considered models on the validation dataset. The identified *black-box* model is able to take into account the phase-lag phenomena presented in Fig. 8.

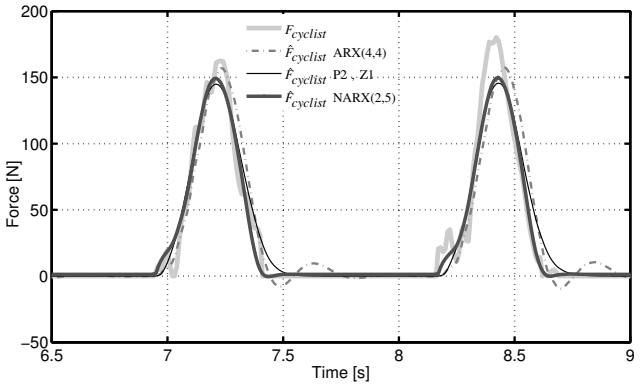

Fig. 9 - Comparison between $F_{cyclist}$ and $\hat{F}_{cyclist}(t)$ considering different models

Note that the open-loop model-based torque reconstruction is viable only for validation in a controlled experimental setting. It is not viable as a operational way of estimating pedaling torque. The model is extremely sensitive to variations of mass, wind, tyre pressure and slope, which are difficultly measured. Current work is focused on developing a closed-loop model-based torque reconstruction.

TABLE I

VALIDATION PERFORMANCE INDEXES FOR DIFFERENT MODEL FAMILIES

$\mathscr{M}$

$\mathscr{M}$	Coefficients	$J_{L_2^2}$ [%]	J_{RMSE} [N]
No model (F_{left})	-	27.0	30.1
Process	2 poles, 1 zero	16.7	17.5
Parametric	ARX(4,4)	17.8	18.1
Non linear	**NARX(2,4)**	**9.1**	**17.1**

V. RESULTS

In this section the NARX(2,4) identified in Section IV is used to validate the algorithms presented in Section III. To do so $\hat{F}_{pedaling}$ (or $\tilde{F}_{pedaling}$) are fed into the NARX(2,4) model, where:

$$\hat{F}_{pedaling} = \hat{T}_{pedaling}\frac{r}{R_w} \quad (19)$$

$$\tilde{F}_{pedaling} = \tilde{T}_{pedaling}\frac{r}{R_w}. \quad (20)$$

The estimated torque is converted in force considering the radius of the rear wheel and the gear ratio. This force is then filtered by the model to obtain $\hat{F}_{cyclist}$ (or $\tilde{F}_{cyclist}$). The estimated force at the rear wheel, $\hat{F}_{cyclist}$ and $\tilde{F}_{cyclist}$, are then compared with $F_{cyclist}$ by means of the performance indexes presented in (17) and (18). A scheme of the evaluation methodology is depicted in Fig. 10.

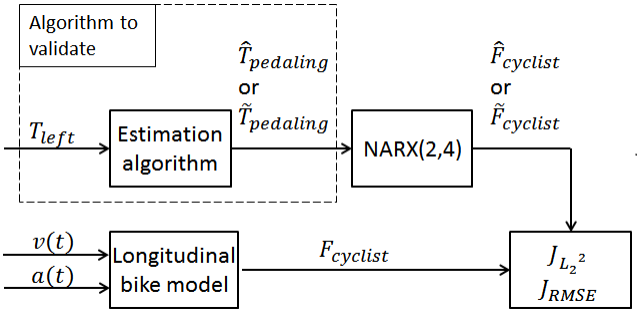

Fig. 10 - The evaluation scheme of the algorithm

Fig. 11 shows a comparison between the reference signal $F_{cyclist}$ and the estimated torque $\hat{F}_{cyclist}$ or $\tilde{F}_{cyclist}$ during a urban cycling test. As one can see:

- There are no major differences between $\hat{F}_{cyclist}$ and $\tilde{F}_{cyclist}$ (see Section III and Fig. 6).
- During "odd" waves (where T_{left} is greater than zero) the measured force and the estimated ones overlap. Indicating that the longitudinal and transmission bike models are reliable enough.
- During "even" waves (where the algorithm estimates $\hat{T}_{right}$ or $\tilde{T}_{right}$) the estimation is less precise. When the pedaling is vigorous and steady the estimation is accurate; however during changes of effort accuracy is lost. For example, near second 6, the symmetry hypotheses break down: the cyclist is delivering less torque/power when pushing with right leg then with the left. In this case the algorithm needs another half revolution to correct the estimate.
- The analysis of the algorithm is more difficult at low forces. The reference force, $F_{cyclist}$, depends on $v(t)$ and $a(t)$ and when the applied force is small the signal-to-noise ratio is not high enough to generate a reliable reference; however the reconstruction algorithm yields consistent results.

All the above observations influence the performance indexes calculated for a urban cycling test of 300 seconds (Table II).

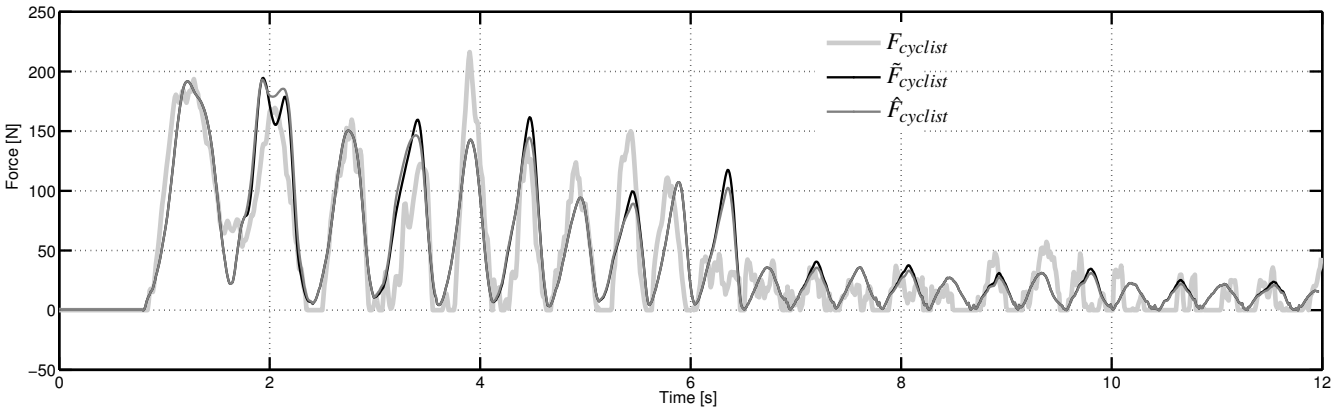

Fig. 11 - Comparison between $F_{cyclist}$, $\hat{F}_{cyclist}$ and $\tilde{F}_{cyclist}$

TABLE II
PERFORMANCE INDEXES $J_{L_2^2}$ AND J_{RMSE} FOR A 300 SECONDS TEST

Index	Symmetry	Value
$J_{L_2^2}$	Power	21.2%
$J_{L_2^2}$	Torque	21.4%
$J_{L_{RMSE}}$	Power	23.8 [N]
$J_{L_{RMSE}}$	Torque	23.9 [N]

Both algorithms estimate pedaling torque with an error of 21%. This error is due to the frequent start and stops during urban cycling; these conditions are particularly challenging from the symmetry approximations point of view. In this context no significant difference has been found between the symmetric power and torque approaches; this gives the opportunity to implement the version that requires less computational efforts (*i.e.* $\hat{T}_{cyclist}$).

Considering the current use of torque information in EPACs for electric torque reference generation, the proposed algorithm is sufficient for estimating cyclist's torque. As a matter of fact, the vast majority of commercial EPACs base their electrical power assistance on an average or filtered value of the cyclist torque. The proposed algorithm has the advantage that at most it has half a revolution of delay, while the filter based techniques suffer from longer lags.

For more other applications, such as control strategies for the regularization of pedaling torque to compensate for the torque dips when the pedal crank is vertical) further investigation is needed to improve accuracy.

VI. CONCLUSIONS

In this work a commercial torque sensor widely use in high-end EPACs has been analyzed. The sensor measures only the left pedaling torque. As a consequence, a technique for evaluating the total pedaling torque is needed. Two algorithms have been proposed and evaluated. They are based on either an iso-power or iso-torque approximation. The algorithms are validated using an accurately calibrated open-loop model-based torque estimation method.

During urban cycling, the algorithms are capable of estimating the pedaling torque with a 21-22 % error. The estimation error is due to the hypothesis of global symmetry of pedaling behavior. The reached level of accuracy is suitable for torque-assisted EPAC's, but may require improvement for other applications. Work is currently carried out to develop closed-loop torque estimation methods in the attempt to improve the accuracy and/or simplify sensor layout.

REFERENCES

[1] A. Muetze and Y. Tan, "Electric bicycles - a performance evaluation," *Industry Applications Magazine, IEEE*, vol. 13, pp. 12 –21, july-aug. 2007.

[2] P. Lataire, J. Timmermans, G. Maggetto, P. Van den Bossche, *et al.*, "Electrically assisted cycling around the world," in *20 th International Electric VehicleSymposium (EVS 20)*, 2003.

[3] P. Spagnol, G. Alli, C. Spelta, P. Lisanti, F. Todeschini, S. M. Savaresi, and A. Morelli, "A full hybrid electric bike: How to increase human efficiency," in *American Control Conference (ACC), 2012*, pp. 2761–2766, June 2012.

[4] P. Spagnol and M. Corno, "Self-sustaining strategy for a hybrid electric bike," in *Submitted to American Control Conference (ACC), 2013*, June 2013.

[5] C. Lin, C. Tsai, and H. Tsai, "An observer for the bicycle pedaling torque and consumed energy estimation," *Journal of Technology*, vol. 23, no. 4, pp. 209–216, 2008.

[6] S. Capmal and H. Vandewalle, "Torque-velocity relationship during cycle ergometer sprints with and without toe clips," *European Journal of Applied Physiology and Occupational Physiology*, vol. 76, pp. 375–379, 1997. 10.1007/s004210050264.

[7] P. Soden and B. Adeyefa, "Forces applied to a bicycle during normal cycling," *Journal of Biomechanics*, vol. 12, no. 7, pp. 527 – 541, 1979.

[8] S. Brand, N. Ertugrul, and W. Soong, "Investigation of an electric assisted bicycle and determination of performance characteristics," in *Australasian Universities Power Engineering Conference*, pp. 1–6, 2003.

[9] G. Alli, S. Formentin, and S. Savaresi, "On the suitability of epacs in urban use," in *Mechatronic Systems*, pp. 277–284, 2010.

[10] L. Ljung, *System identification: theory for the user*. Prentice-Hall Englewood Cliffs, NJ, 1987.